

Charged bottomonium-like structures in the hidden-bottom dipion decays of $\Upsilon(11020)$

Dian-Yong Chen^{1,3,*}, Xiang Liu^{1,2,†,‡} and Takayuki Matsuki^{1,2,4,§}

¹Research Center for Hadron and CSR Physics, Lanzhou University and Institute of Modern Physics of CAS, Lanzhou 730000, China

²School of Physical Science and Technology, Lanzhou University, Lanzhou 730000, China

³Nuclear Theory Group, Institute of Modern Physics of CAS, Lanzhou 730000, China

⁴Tokyo Kasei University, 1-18-1 Kaga, Itabashi, Tokyo 173, JAPAN

(Dated: June 21, 2018)

Under the Initial Single Pion Emission mechanism, we study the hidden-bottom dipion decays of $\Upsilon(11020)$, i.e., $\Upsilon(11020) \rightarrow \Upsilon(nS)\pi^+\pi^-$ ($n = 1, 2, 3$) and $\Upsilon(11020) \rightarrow h_b(mP)\pi^+\pi^-$ ($m = 1, 2$). We predict explicit sharp peak structures close to the $B\bar{B}^*$ and $B^*\bar{B}$ thresholds and their reflections in the $\Upsilon(1S)\pi^+$, $\Upsilon(2S)\pi^+$ and $h_b(1P)\pi^+$ invariant mass spectrum distributions. We suggest future experiment, i.e., Belle, BaBar, and forthcoming BelleII or Super-B, carry out the search for these novel phenomena, which can provide important test to the Initial Single Emission mechanism existing in higher bottomonia.

PACS numbers: 13.25.Gv, 14.40.Pq, 13.75.Lb

Recently we have proposed a new decay mechanism, Initial Single Pion Emission (ISPE) [1], existing in the hidden-bottom dipion decays of $\Upsilon(5S)$. By the ISPE mechanism, we have succeeded in producing two charged bottomonium-like structures in the $\Upsilon(nS)\pi^\pm$ ($n = 1, 2, 3$) and $h_b(mP)\pi^\pm$ ($m = 1, 2$) invariant mass spectrum distributions [1], which are above the $B\bar{B}^*$ and $B^*\bar{B}$ thresholds, respectively. What is most important is that these peak structures appear exactly at the energies corresponding to two charged $Z_b(10610)$ and $Z_b(10650)$ newly observed by the Belle Collaboration [2]. In our previous work [3], we introduced the intermediate $Z_b(10610)$ and $Z_b(10650)$ contribution to the $\Upsilon(5S)$ hidden-bottom dipion decay, where we have solved the puzzling on the $\cos\theta$ distribution of $\Upsilon(5S) \rightarrow \Upsilon(2S)\pi^+\pi^-$ given by Belle [4]. To some extent, the work presented in Ref. [1] adopted different assumptions compared with Ref. [3].

Following Ref. [1], we have applied the ISPE mechanism to the hidden-charm dipion decays of $\psi(4040)$, $\psi(4160)$, $\psi(4415)$, and $Y(4260)$, and two charged charmonium-like structures are predicted close to the $D\bar{D}^*$ and $D^*\bar{D}$ thresholds [5]. The predicted line shape of $d\Gamma/dm_{h_c(1P)\pi}$ of $\psi(4160) \rightarrow h_c(1P)\pi^+\pi^-$ can explain the CLEO-c measurement of the $h_c(1P)\pi^\pm$ invariant mass distribution from $e^+e^- \rightarrow h_c(1P)\pi^+\pi^-$ at $E_{CM} = 4170$ MeV [6].

If the ISPE mechanism is a universal one in the hidden-bottom dipion decays of heavy quarkonia, we can naturally apply this to study the decay behaviors of other higher bottomonia, and predict some novel phenomena. In Fig. 1, we present the mass spectra of bottomonia with $J^{PC} = 1^{--}$ [7], which are usually named as the Υ family. The comparison of Υ states with the $B\bar{B}$ threshold indicates that there are only three bottomonia just above the $B\bar{B}$ threshold. Other than $\Upsilon(10860)$ studied in Ref. [1], $\Upsilon(11020)$ can serve a good testing ground to study the hidden-bottom dipion decay involving

the ISPE mechanism, where $\Upsilon(11020)$ was first observed by the CUSB Collaboration [8] and the CLEO Collaboration [9], and measured again by BaBar recently [10].

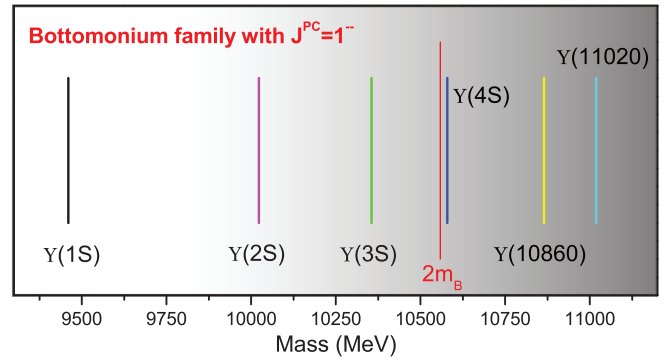


FIG. 1: (Color online.) The mass spectrum of Υ family. Here, we also list the threshold of $B\bar{B}$ and make a comparison with Υ states.

Because the mass of $\Upsilon(11020)$ is above the sum of the masses of the emitted π and the intermediate $B^{(*)} + \bar{B}^{(*)}$, the pion initially emitted by $\Upsilon(11020)$ plays a crucial role to make $B^{(*)}$ and $\bar{B}^{(*)}$ have low momenta, which can easily interact with each other to transit into final states. This picture is named as the ISPE mechanism [1]. In Fig. 2, we give the schematic diagrams for the hidden-bottom dipion decay of $\Upsilon(11020)$.

In this letter, the hidden-bottom dipion decays of $\Upsilon(11020)$ include

$$\Upsilon(11020) \Rightarrow \pi^\pm + \begin{cases} \{B\bar{B}\}^\mp \\ \{B\bar{B}^* + B^*\bar{B}\}^\mp \\ \{B^*\bar{B}^*\}^\mp \end{cases} \Rightarrow \begin{cases} \Upsilon(1S)\pi^+\pi^- \\ \Upsilon(2S)\pi^+\pi^- \\ \Upsilon(3S)\pi^+\pi^- \\ h_b(1P)\pi^+\pi^- \\ h_b(2P)\pi^+\pi^- \end{cases}, \quad (1)$$

where $B\bar{B}$, $B\bar{B}^* + B^*\bar{B}$, and $B^*\bar{B}^*$ are the intermediate states contributing to the triangle loops. The superscript \pm or \mp denotes the charges of pion or $B^{(*)}\bar{B}^{(*)}$ pair. Diagrams (a) and

*Corresponding author

†Electronic address: chendy@impcas.ac.cn

‡Electronic address: xiangliu@lzu.edu.cn

§Electronic address: matsuki@tokyo-kasei.ac.jp

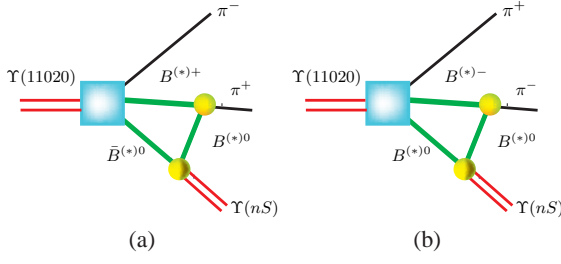


FIG. 2: The schematic hadron-level diagrams relevant to hidden-bottom dipion decay of $\Upsilon(11020)$ due to the ISPE mechanism. By replacing $\Upsilon(nS)$ with $h_b(mP)$ in the final state, we obtain the schematic diagrams for $\Upsilon(11020) \rightarrow h_b(mP)\pi^+\pi^-$.

(b) shown in Fig. 2 can be transformed into each other if considering particle and antiparticle conjugation $B^{(*)} \rightleftharpoons \bar{B}^{(*)}$ and $\pi^+ \rightleftharpoons \pi^-$. By interchanging $B^{(*)+} \rightleftharpoons B^{(*)0}$, $B^{(*)-} \rightleftharpoons \bar{B}^{(*)0}$, and $\pi^+ \rightleftharpoons \pi^-$, one can deduce other diagrams relevant to the hidden-bottom dipion decay of $\Upsilon(11020)$. We find that there exist 4, 12, and 8 diagrams for $\Upsilon(11020) \rightarrow \Upsilon(nS)\pi^+\pi^-$ decay via intermediate $B\bar{B}$, $B\bar{B}^* + B^*\bar{B}$, and $B^*\bar{B}^*$, respectively, and 4, 8, and 8 diagrams for $\Upsilon(11020) \rightarrow h_b(mP)\pi^+\pi^-$ via intermediate $B\bar{B}$, $B\bar{B}^* + B^*\bar{B}$, and $B^*\bar{B}^*$, respectively (see Ref. [5] for more details).

Because we use hadron-level description to the hidden-bottom dipion decays of $\Upsilon(11020)$, the effective Lagrangian approach is an appropriate way to describe the decay amplitudes relevant to this process. The effective interaction Lagrangians involved in our calculation are given by, [11–14]

$$\begin{aligned} \mathcal{L}_{\Upsilon(11020)B^{(*)}B^{(*)}\pi} = & \\ & -ig_{\Upsilon B\pi} \epsilon^{\mu\nu\alpha\beta} \Upsilon_\mu^\nu \partial_\nu B \partial_\alpha \pi \partial_\beta \bar{B} + g_{\Upsilon B^*\pi} \Upsilon^{\mu\nu} (B\pi \bar{B}_\mu^* + B_\mu^* \pi \bar{B}) \\ & -ig_{\Upsilon B^*\pi} \epsilon^{\mu\nu\alpha\beta} \Upsilon_\mu^\nu \partial_\nu B^* \partial_\alpha \pi \bar{B}_\beta^* - ih_{\Upsilon B^*\pi} \epsilon^{\mu\nu\alpha\beta} \partial_\mu \Upsilon_\nu^\alpha \pi \bar{B}_\beta^*, \end{aligned} \quad (2)$$

$$\begin{aligned} \mathcal{L}_{B^*B^*\pi} = & \\ & ig_{B^*B\pi} (B_\mu^* \partial^\mu \pi \bar{B} - B \partial^\mu \pi \bar{B}_\mu^*) - g_{B^*B^*\pi} \epsilon^{\mu\nu\alpha\beta} \partial_\mu B_\nu^* \pi \partial_\alpha \bar{B}_\beta^*, \end{aligned} \quad (3)$$

$$\begin{aligned} \mathcal{L}_{\Upsilon(nS)B^{(*)}B^{(*)}} = & \\ & ig_{\Upsilon BB} \Upsilon_\mu (\partial^\mu B \bar{B} - B \partial^\mu \bar{B}) - g_{\Upsilon B^*B} \epsilon^{\mu\nu\alpha\beta} \partial_\mu \Upsilon_\nu (\partial_\alpha B_\beta^* \bar{B} \\ & + B \partial_\alpha \bar{B}_\beta^*) - ig_{\Upsilon B^*\pi} \left\{ \Upsilon^\mu (\partial_\mu B^{*\nu} \bar{B}_\nu^* - B^{*\nu} \partial_\mu \bar{B}_\nu^*) \right. \\ & \left. + (\partial_\mu \Upsilon_\nu B^{*\nu} - \Upsilon_\nu \partial_\mu B^{*\nu}) \bar{B}^{*\mu} + B^{*\mu} (\Upsilon^\nu \partial_\mu \bar{B}_\nu^* - \partial_\mu \Upsilon^\nu \bar{B}_\nu^*) \right\}, \end{aligned} \quad (4)$$

$$\begin{aligned} \mathcal{L}_{h_b(mP)B^{(*)}B^{(*)}} = & \\ & gh_b B^* h_b^\mu (B\bar{B}_\mu^* + B_\mu^* \bar{B}) + ig_{h_b B^* B^*} \epsilon^{\mu\nu\alpha\beta} \partial_\mu h_{b\nu} B_\alpha^* \bar{B}_\beta^* \end{aligned} \quad (5)$$

with $\pi = \vec{\tau} \cdot \vec{\pi}$. In addition, we take $B^{(*)} = (B^{(*)+}, B^{(*)0})$ and $\bar{B}^{(*)T} = (B^{(*)-}, \bar{B}^{(*)0})$, which correspond to the bottom meson isodoublets. These effective Lagrangians presented in Eqs. (2)-(4) can be strictly derived, terms including epsilon tensor from Ref. [11] and other terms from Ref. [12], by extending the symmetry from $SU(4)$ to $SU(5)$. Here, the four-point vertex $\Upsilon(11020)B^{(*)}\bar{B}^{(*)}\pi$ is described by Eq. (2). The first term in Eq. (2) is similar to the effective Lagrangian de-

scribing $\omega \rightarrow [\pi + \rho]_{L=1}$, except for the replacement of ρ by an anti-symmetric combination of two fields corresponding to the B and \bar{B} mesons. Thus, $\Upsilon\pi BB$ can be simplified as a $1^- \rightarrow [0^- + 1^-]_{L=1}$ basic process. The second term in Eq. (2) reflects $1^- \rightarrow 0^- + [0^- + 1^-]_{L=0}$, while the third term in Eq. (2) is a $1^- \rightarrow \{0^- + [1^- + 1^-]_{L=1}\}_{L=1}$ process. In Eq. (2), the fourth term is same as the third term, except for parity violation coupling to $B^*B^*\pi$ due to the $V - A$ interaction. Eq. (3) corresponds to the couplings of $B^{(*)}$ and $\bar{B}^{(*)}$ mesons with pion, which are P-wave interactions, i.e., $B^{(*)} \rightarrow [B^{(*)} + \pi]_{L=1}$. Eqs. (4) and (5) show the interaction of bottomonia $\Upsilon(nS)$ and $h_b(mP)$ with $B^{(*)}$ and $\bar{B}^{(*)}$ mesons, respectively, where $\Upsilon(nS) \rightarrow [B^{(*)} + \bar{B}^{(*)}]_{L=1}$ interactions are typical P-wave couplings, while $h_b(mP) \rightarrow [B^{(*)} + \bar{B}^{(*)}]_{L=0}$ are S-wave interactions. In the explanation presented above, the subscripts $L = 0$ and $L = 1$ denote the interactions of the subsystems in the brackets [...] and {...} being S-wave and P-wave couplings, respectively. The coupling constants in Eq. (3) satisfy the relation $g_{B^*B^*\pi} = \frac{g_{B^*B\pi}}{\sqrt{m_B m_{B^*}}} = \frac{2g}{f_\pi}$. By using the branching ratio of $D^* \rightarrow D\pi$ measured by CLEO-c [15] and $f_\pi = 132$ MeV, one gets $g = 0.59$ [16]. In Eq. (4), there also exists the relation

$$g_{\Upsilon BB} = g_{\Upsilon B^* B^*} \frac{m_B}{m_{B^*}} = g_{\Upsilon B^* B^*} m_\Upsilon \sqrt{\frac{m_B}{m_{B^*}}} = \frac{m_\Upsilon}{f_\Upsilon},$$

where f_Υ and m_Υ denote the decay constant and the mass of $\Upsilon(nS)$, respectively. In addition, the coupling constants in Eq. (5) are determined as

$$g_{h_b BB^*} = -2g_1 \sqrt{m_{h_b} m_B m_{B^*}}, \quad g_{h_b B^* B^*} = 2g_1 \frac{m_{B^*}}{\sqrt{m_{h_b}}}, \quad (6)$$

with $g_1 = -\sqrt{\frac{m_{\chi_{b0}}}{3}} \frac{1}{f_{\chi_{b0}}}$, where $m_{\chi_{b0}}$ and $f_{\chi_{b0}}$ are the mass and the decay constant of $\chi_{b0}(1P)$, respectively [14].

Taking the process $\Upsilon(11020) \rightarrow \pi^\pm \{B\bar{B}\}^\mp \rightarrow \Upsilon(nS)\pi^+\pi^-$, $h_b(mP)\pi^+\pi^-$ as an example, we illustrate how to deduce the corresponding decay amplitudes. In Fig. 3, the ISPE mechanism gives the hadron-level diagrams depicting $\Upsilon(11020) \rightarrow \pi^\pm \{B\bar{B}\}^\mp \rightarrow \Upsilon(nS)\pi^+\pi^-$. We can easily obtain the diagrams for $\Upsilon(11020) \rightarrow \pi^\pm \{B\bar{B}\}^\mp \rightarrow h_b(mP)\pi^+\pi^-$ by replacing $\Upsilon(nS)$ with $h_b(mP)$.

The decay amplitude of Fig. 3 (a) can be written as

$$\begin{aligned} \mathcal{M}_a = & (i)^3 \int \frac{d^4 q}{(2\pi)^4} [-ig_{\Upsilon B\pi} \epsilon_{\mu\nu\alpha\beta} \epsilon_\nu^\mu (ip_1^\alpha) (ip_3^\beta) (ip_2^\gamma)] \\ & \times [ig_{B^*B\pi} (-ip_4^\lambda)] [-g_{\Upsilon(nS)B^*B} \epsilon_{\delta\theta\phi} (ip_3^\delta) \epsilon_{\Upsilon(nS)}^\nu (-iq^\theta)] \\ & \times \frac{1}{p_1^2 - m_B^2} \frac{1}{p_2^2 - m_B^2} \frac{-g_{\lambda\phi} + q_\lambda q_\phi / m_{B^*}^2}{q^2 - m_{B^*}^2} \mathcal{F}^2(q^2), \end{aligned} \quad (7)$$

or

$$\begin{aligned} \mathcal{M}_a = & (i)^3 \int \frac{d^4 q}{(2\pi)^4} [-ig_{\Upsilon B\pi} \epsilon_{\mu\nu\alpha\beta} \epsilon_\nu^\mu (ip_1^\alpha) (ip_3^\beta) (ip_2^\gamma)] \\ & \times [ig_{B^*B\pi} (-ip_{4,\lambda})] [-g_{h_b B^* B^*} \epsilon_{h_b}^\nu] \frac{1}{p_1^2 - m_B^2} \frac{1}{p_2^2 - m_B^2} \\ & \times \frac{-g^{\lambda\nu} + q^\lambda q^\nu / m_{B^*}^2}{q^2 - m_{B^*}^2} \mathcal{F}^2(q^2), \end{aligned} \quad (8)$$

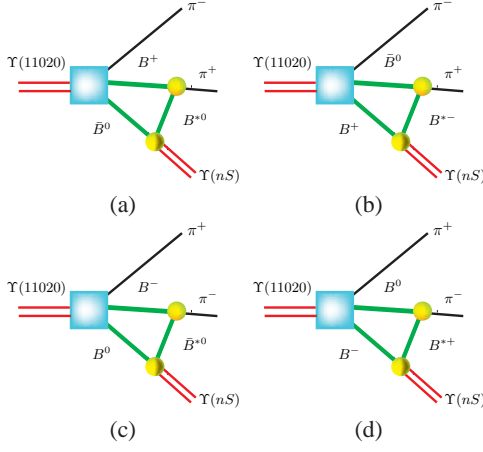


FIG. 3: (Color Online) The hadron-level diagrams for $\Upsilon(11020) \rightarrow \Upsilon(nS)\pi^+\pi^-$ ($n = 1, 2, 3$) decays with $B\bar{B}$ as the intermediate states. Replacing $\Upsilon(nS)$ with $h_b(mP)$, we get all diagrams for $\Upsilon(11020) \rightarrow h_b(mP)\pi^+\pi^-$ decays.

which corresponds to the process

$$\Upsilon(11020) \rightarrow \pi^- B^+(p_1)\bar{B}^0(p_2) \rightarrow \Upsilon(nS)(p_3)\pi^+(p_4)\pi^-(p_5),$$

or

$$\Upsilon(11020) \rightarrow \pi^- B^+(p_1)\bar{B}^0(p_2) \rightarrow h_b(mP)(p_3)\pi^+(p_4)\pi^-(p_5),$$

where q denotes the momentum of the exchanged meson B^{*0} in transition $B^+\bar{B}^0 \rightarrow \Upsilon(nS)\pi^+\pi^-$. We take $\mathcal{F}(q^2) = (\Lambda^2 - m_{B^*}^2)/(q^2 - m_{B^*}^2)$, which denotes the monopole form factor to describe the vertex structure appearing in the $B\bar{B} \rightarrow \Upsilon(nS)\pi^+$ transition. In addition, such form factor also plays an important role to compensate the off-shell effect of the exchanged $B^{(*)}$ mesons. In general, the cutoff Λ can be parameterized as $\Lambda = \xi\Lambda_{QCD} + m_{B^*}$ with $\Lambda_{QCD} = 220$ MeV. The decay amplitude of Fig. 3 (c) is given by Eq. (7) or Eq. (8) by interchanging p_4 and p_5 with each other, i.e.,

$$\mathcal{M}_c = \mathcal{M}_a|_{p_5 \rightarrow p_4}^{p_4 \rightarrow p_5}.$$

Due to $SU(2)$ symmetry, we find other relations of the decay amplitudes

$$\mathcal{M}_b = \mathcal{M}_a, \quad \mathcal{M}_d = \mathcal{M}_c, \quad (9)$$

where decay amplitudes \mathcal{M}_i ($i = a, b, c, d$) correspond to Fig. 3 (i). Eq. (9) make the total decay amplitudes of $\Upsilon(11020) \rightarrow \Upsilon(nS)\pi^+\pi^-$ and $\Upsilon(11020) \rightarrow h_b(mP)\pi^+\pi^-$ be simplified as

$$\mathcal{M} = 2(\mathcal{M}_a + \mathcal{M}_c), \quad (10)$$

where the factor 2 reflects the $SU(2)$ symmetry just considered in this letter. In Ref. [5], we have listed the detailed diagrams and formulation of the hidden-charm dipion decays of higher charmonia, where we consider the intermediate $D\bar{D}^* + D^*\bar{D}$ and $D^*\bar{D}^*$ contributions to higher charmonium decays by the ISPE mechanism. Thus, replacing {initial higher charmonium $\rightarrow \Upsilon(11020)$ } and $\{D^{(*)}/\bar{D}^{(*)} \rightarrow \bar{B}^{(*)}/B^{(*)}\}$, one

TABLE I: A summary of mass adopted in this letter.

Mass (MeV) [7]					
$\Upsilon(11020)$	$\Upsilon(3S)$	$\Upsilon(2S)$	$\Upsilon(1S)$	$h_b(1P)$ [17]	$h_b(2P)$ [17]
11019	10355	10023	9460	9898	10259
B	B^*	π			
5279	5325	140			

can obtain the corresponding decay amplitudes for $\Upsilon(11020)$ hidden-bottom dipion decays via the intermediate $B\bar{B}^* + B^*\bar{B}$ and $B^*\bar{B}^*$ (see Ref. [5] for more details).

With the above prescription, the differential decay width for $\Upsilon(11020)$ decay into $\Upsilon(nS)\pi^+\pi^-$ reads as

$$d\Gamma = \frac{1}{(2\pi)^3} \frac{1}{32m_{\Upsilon(11020)}^3} \overline{|\mathcal{M}|^2} dm_{\Upsilon(nS)\pi^+}^2 dm_{\pi^+\pi^-}^2 \quad (11)$$

with $m_{\Upsilon(nS)\pi^+}^2 = (p_4 + p_5)^2$ and $m_{\pi^+\pi^-}^2 = (p_3 + p_4)^2$, where the overline indicates the average over the polarizations of the $\Upsilon(11020)$ in the initial state and the sum over the polarization of $\Upsilon(nS)$ in the final state. Replacing $m_{\Upsilon(nS)\pi^+}$ with $m_{h_b(mP)\pi^+}$, we obtain the differential decay width for $\Upsilon(11020) \rightarrow h_b(mP)\pi^+\pi^-$. The values of the meson masses involved in the hidden-bottom dipion decays of $\Upsilon(11020)$ are listed in Table. I.

In Fig. 4, we show the dependence of $d\Gamma(\Upsilon(11020) \rightarrow \Upsilon(nS)\pi^+\pi^-)/dm_{\Upsilon(nS)\pi^+}$ and $d\Gamma(\Upsilon(11020) \rightarrow h_b(mP)\pi^+\pi^-)/dm_{h_b(mP)\pi^+}$ on the $\Upsilon(nS)\pi^+$ and $h_b(mP)\pi^+$ invariant mass spectra, respectively, where we take $\xi = 1$. We need to specify that these numerical results listed in Fig. 4 are weakly dependent on the values of the parameter ξ , which is consistent with that found in Ref. [1]. Because we only focus on the line shapes of $d\Gamma(\Upsilon(11020) \rightarrow \Upsilon(nS)\pi^+\pi^-)/dm_{\Upsilon(nS)\pi^+}$ and $d\Gamma(\Upsilon(11020) \rightarrow h_b(mP)\pi^+\pi^-)/dm_{h_b(mP)\pi^+}$, the maxima of the line shapes in Fig. 4 are normalized to be 1.

Our theoretical calculation indicates (1) there exist explicit sharp peaks close to the $B\bar{B}^*$ and $B^*\bar{B}^*$ thresholds in the $\Upsilon(1S)\pi^+$, $\Upsilon(2S)\pi^+$, and $h_b(1P)\pi^+$ invariant mass spectrum distributions. In addition, we also find the reflections of these sharp peaks on the lower side of the invariant mass; (2) the broad structures close to the $B\bar{B}^*$ and $B^*\bar{B}^*$ thresholds appear in the $\Upsilon(3S)\pi^+$ invariant mass spectrum distribution, which are due to the overlapping peaks of two corresponding reflections; (3) in the $h_b(2P)\pi^+$ invariant mass spectrum, we also find a structure around $B\bar{B}^*$ threshold, which is narrower than that appearing in the $\Upsilon(3S)\pi^+$ invariant mass spectrum. In addition, we also find a small peak around $B^*\bar{B}^*$ and its reflection, which are close to each other; (4) the intermediate $B\bar{B}$ contribution to the hidden-bottom dipion decays of $\Upsilon(11020)$ does not give the phenomena similar to those from the intermediate $B\bar{B}^*$ and $B^*\bar{B}^*$ states contributing to $\Upsilon(11020)$ decays just described above. They just give broad background-like line shape.

When comparing the results shown in Fig. 4 with those of Figs. 3-4 in Ref. [1], we notice the differences between these results, which are mainly due to the change of mass of the initial state, i.e., the mass of $\Upsilon(11020)$ is different from that of $\Upsilon(5S)$ (10860 MeV).

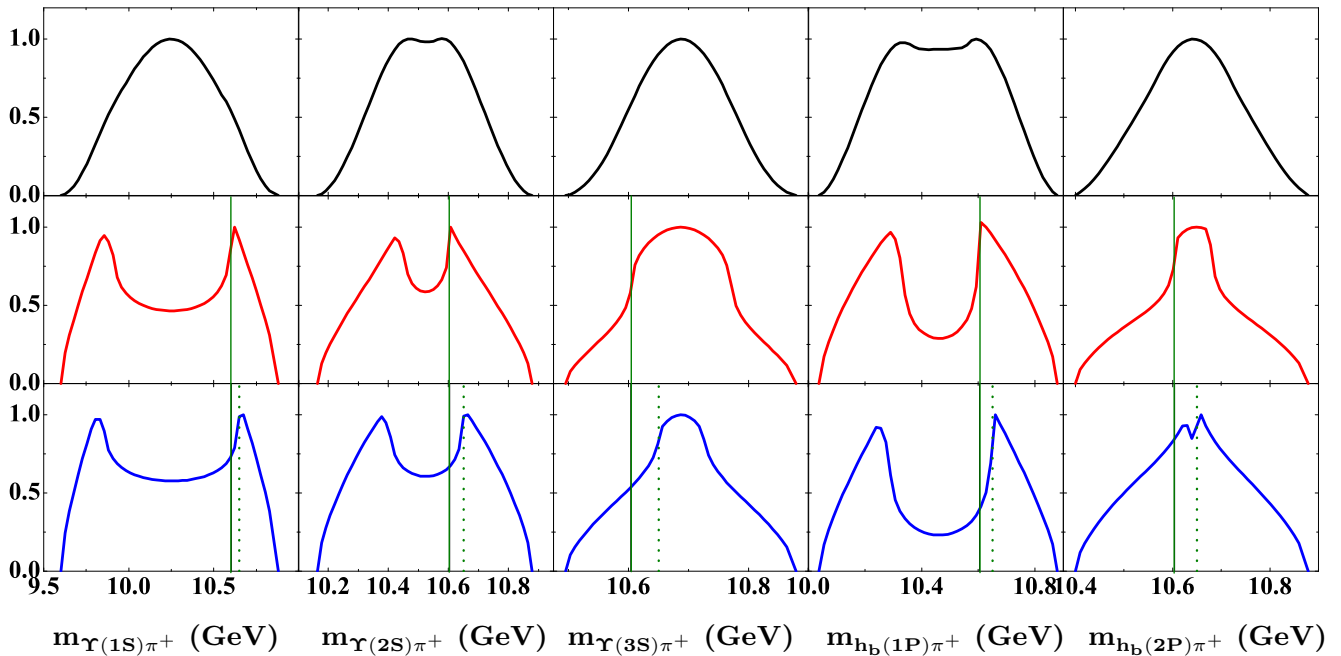


FIG. 4: (Color online.) The distribution of $d\Gamma(\Upsilon(11020) \rightarrow \Upsilon(nS)\pi^+\pi^+)/dm_{\Upsilon(nS)\pi^+}$ and $d\Gamma(\Upsilon(11020) \rightarrow h_b(mP)\pi^+\pi^+)/dm_{h_b(mP)\pi^+}$ dependent on the $\Upsilon(nS)\pi^+$ and $h_b(mP)\pi^+$ invariant mass spectra. Here, the results presented in the first, the second, and the third rows are from the intermediate $B\bar{B}$, $B\bar{B}^* + B^*\bar{B}$, and $B^*\bar{B}^*$ contributions, respectively. The vertical solid and dashed lines denote the threshold of $B\bar{B}^* + B^*\bar{B}$ and $B^*\bar{B}^*$, respectively.

The comparison of line shapes in Fig. 4 indicates that the line shapes are dependent on the definite hidden-bottom dipion decays of $\Upsilon(11020)$. Although we have obtained the peak structures just shown in Fig. 4, these are not typical Breit-Wigner type distributions when subtracting the contribution from the reflection. Thus, use of mass and width to specify these peak structures is not appropriate and realistic. In this work, we would like to emphasize that the sharp peak structures appear in the corresponding invariant mass spectrum, which can be tested in future experiment.

In conclusion, in this letter we study the hidden-bottom dipion decays of $\Upsilon(11020)$ by the ISPE mechanism, which has been first proposed in Ref. [1] to study two charged Z_b structures observed by Belle [2] and has also been applied to investigate the hidden-charm dipion decays of higher charmonia [5]. Furthermore, we predict the charged bottom-like structures close to the $B\bar{B}^*$ and $B^*\bar{B}^*$ thresholds, which exist in the $\Upsilon(nS)\pi^\pm$ and $h_b(mP)\pi^\pm$ invariant mass spectra of the hidden-bottom dipion decays of $\Upsilon(11020)$. Just indicated in this letter, these charged peak structures are predicted due to the ISPE mechanism, a peculiar effect involved in the decays of higher bottomonia and/or charmonia [1, 5]. We must admit that there exists interference between background and the ISPE contributions, where in this work we do not include background contribution due to our ignorance to background contribution. To some extent, such interference effect could bring some uncertainty to our prediction.

At present, there only exist the experimental measurements of the mass and width for $\Upsilon(11020)$ [8–10] while the infor-

mation of its strong decay behaviors is still absent [7]. To some extent, the prediction presented in this letter could stimulate experimentalists' interest in carrying out further study on $\Upsilon(11020)$, especially on its hidden-bottom dipion decays. Besides Belle and BaBar, the forthcoming Belle II experiment [18] will provide a good platform to study the properties of $\Upsilon(11020)$. In addition, the SuperB Factory has been approved by the Italian government in the last year [19], which is also suitable to study the bottomonium decays. Here, we suggest these experimental search for the predicted charged bottomonium-like structures around the $B\bar{B}^*$ and $B^*\bar{B}^*$ thresholds by the hidden-bottom dipion decays of $\Upsilon(11020)$, which will provide a crucial test on the ISPE mechanism [1].

Acknowledgments

This project is supported by the National Natural Science Foundation of China under Grants Nos. 11175073, No. 11005129, No. 11035006, No. 11047606, the Ministry of Education of China (FANEDD under Grant No. 200924, DP-FIHE under Grant No. 20090211120029, NCET under Grant No. NCET-10-0442, the Fundamental Research Funds for the Central Universities), and the West Doctoral Project of Chinese Academy of Sciences. One of the authors (TM) would like to sincerely thank Prof. Xiang Liu for his kind hospitality during the course of this work.

-
- [1] D. Y. Chen and X. Liu, arXiv:1106.3798 [hep-ph].
- [2] I. Adachi *et al.* [Belle Collaboration], arXiv:1105.4583 [hep-ex].
- [3] D. Y. Chen, X. Liu and S. L. Zhu, arXiv:1105.5193 [hep-ph].
- [4] K. F. Chen *et al.* [Belle Collaboration], Phys. Rev. Lett. **100**, 112001 (2008) [arXiv:0710.2577 [hep-ex]].
- [5] D. Y. Chen and X. Liu, Phys. Rev. **D84**, 034032 (2011) [arXiv:1106.5290 [hep-ph]].
- [6] T. K. Pedlar *et al.* [CLEO Collaboration], Phys. Rev. Lett. **107**, 041803 (2011) [arXiv:1104.2025 [hep-ex]].
- [7] K. Nakamura *et al.* [Particle Data Group], J. Phys. G **37**, 075021 (2010).
- [8] D. M. J. Lovelock *et al.*, Phys. Rev. Lett. **54**, 377 (1985).
- [9] D. Besson *et al.* [CLEO Collaboration], Phys. Rev. Lett. **54**, 381 (1985).
- [10] B. Aubert *et al.* [BABAR Collaboration], Phys. Rev. Lett. **102**, 012001 (2009) [arXiv:0809.4120 [hep-ex]].
- [11] O. Kaymakcalan, S. Rajeev, J. Schechter, Phys. Rev. **D30**, 594 (1984).
- [12] Y. S. Oh, T. Song and S. H. Lee, Phys. Rev. C **63**, 034901 (2001) [arXiv:nucl-th/0010064].
- [13] R. Casalbuoni, A. Deandrea, N. Di Bartolomeo, R. Gatto, F. Feruglio and G. Nardulli, Phys. Rept. **281**, 145 (1997) [arXiv:hep-ph/9605342].
- [14] P. Colangelo, F. De Fazio and T. N. Pham, Phys. Lett. B **542**, 71 (2002) [arXiv:hep-ph/0207061].
- [15] A. Anastassov *et al.* [CLEO Collaboration], Phys. Rev. D **65**, 032003 (2002) [arXiv:hep-ex/0108043].
- [16] C. Isola, M. Ladisa, G. Nardulli and P. Santorelli, Phys. Rev. D **68**, 114001 (2003) [arXiv:hep-ph/0307367].
- [17] I. Adachi *et al.* [Belle Collaboration], arXiv:1103.3419 [hep-ex].
- [18] <http://epp.physics.unimelb.edu.au/Belle/The-Belle-II-Experiment>.
- [19] <http://web.infn.it/superb/>.